THE ASTROPHYSICAL JOURNAL, 546:L57–L60, 2001 January 1

OBSERVABILITY OF STELLAR WINDS FROM LATE-TYPE DWARFS VIA CHARGE EXCHANGE X-RAY EMISSION

BRADFORD J. WARGELIN AND JEREMY J. DRAKE
Harvard-Smithsonian Center for Astrophysics, 60 Garden Street, Cambridge, MA 02138; bwargelin@cfa.harvard.edu
Received 2000 September 16; accepted 2000 October 25; published 2000 December 29

ABSTRACT

Despite the fact that the overwhelming majority of stars are of late spectral type (F–M) and lie on the main sequence, we know nothing about their stellar winds. Existing measurements of winds only apply to high-mass O and B stars, red giants, and supergiants and only extend down to a few times $10^{-10}\ M_\odot\ \mathrm{yr}^{-1}$, as compared to the solar rate of $\sim 2 \times 10^{-14}\ M_\odot\ \mathrm{yr}^{-1}$. Attempts to detect winds from late-type dwarf stars have to date resulted only in loose upper limits of order 10^{-12} to $10^{-11}\ M_\odot\ \mathrm{yr}^{-1}$. We propose a novel method of studying stellar winds through observation of charge exchange–induced X-ray emission. Recent X-ray detections of comets suggest that charge transfer between highly charged ions in the solar wind and neutral gases in cometary atmospheres is responsible for much or all of the observed emission, a hypothesis that has been strengthened by *Chandra* observations of comet C/1999 S4 (LINEAR). It has also been proposed that charge transfer between the solar wind and the local interstellar medium (ISM) produces a substantial fraction of the soft X-ray background observed by *ROSAT* and various rocket experiments. We show that the same process may be observable in nearby dwarf star systems using *Chandra* and future large-area high-resolution observatories, which would provide hitherto unobtainable information on wind geometry, ion composition, mass-loss rates, and the distribution of neutral gas in the ISM.

Subject headings: atomic processes — ISM: structure — stars: winds, outflows — X-rays: stars

On-line material: color figures

1. INTRODUCTION

Although it is generally assumed that all stars lose mass via stellar winds, our understanding of that process, even for the Sun, is poor. Current estimates of stellar mass-loss rates rely on measurements of P Cygni profiles, optical and molecular emission lines, IR and radio excesses, and absorption lines in binary systems and range from a few times 10^{-10} to more than $10^{-5}\ M_\odot\ \mathrm{yr}^{-1}$ (Lamers & Cassinelli 1999). These rates, however, apply only for massive OB and Wolf-Rayet stars or cool red giants and supergiants. No data exist for the more modest stellar winds from late-type main-sequence stars such as the Sun, a G2 dwarf that has a mass-loss rate of $\sim 2 \times 10^{-14}\ M_\odot\ \mathrm{yr}^{-1}$, more than four decades lower than the current limit for nonsolar measurements.

Measurements of stellar wind parameters such as mass loss, wind velocity, and ion composition are needed to constrain models of stellar evolution, mass-loss mechanisms, and coronal cooling as well as permit estimates of the rate of element dispersal, kinetic heating, and ionization within the interstellar medium (ISM). The mass-loss rate is of critical importance in models of angular momentum loss in late-type stars, but it has proven very difficult to estimate such properties from theoretical first principles (see, for example, Krishnamurthi et al. 1997).

Another example of the importance of dwarf star winds is the proposal that such winds are responsible for sweeping out the gas and dust ejected by red giants in globular clusters (Coleman & Worden 1977). Recently, Smith (1999) has shown that if all M dwarfs have the same wind velocity and mass-loss rate per unit mass as the Sun, then the resulting outflows are sufficient to strip red giant ejecta from globular clusters, assuming plausible values for the giants' mass-loss rates. The case for cluster gas stripping by dwarfs is made even stronger if one assumes that low-mass flare stars have significantly higher mass-loss rates, as seems plausible (Badalyan & Livshits 1992).

Several authors have argued that main-sequence stars may have mass-loss rates near or just below the current detection threshold of a few times $10^{-10}\ M_\odot\ \mathrm{yr}^{-1}$. Willson, Bowen, & Struck-Marcell (1987) suggested that dwarf A and F stars that lie in the δ Scuti pulsational instability strip might have mass-loss rates between 10^{-9} and $10^{-8}\ M_\odot\ \mathrm{yr}^{-1}$, but Brown et al. (1990) argued that Very Large Array measurements placed much lower limits on the ionized mass-loss rate from such stars and that this mass-loss rate was representative of the total rate.

Mullan et al. (1992) analyzed data from the James Clerk Maxwell Telescope and concluded that flaring M stars might have mass-loss rates of a few times $10^{-10}\ M_\odot\ \mathrm{yr}^{-1}$, but other authors using more detailed models have concluded that the loss rates cannot be higher than a few times $10^{-12}\ M_\odot\ \mathrm{yr}^{-1}$ (Lim & White 1996; van den Oord & Doyle 1997). As we will show, however, even these modest mass-loss rates should be detectable with current and planned X-ray observatories.

2. CHARGE EXCHANGE X-RAYS FROM THE SOLAR WIND

It has been known for decades that charge exchange (CX) occurs between solar wind ions and neutral gas in the ISM, but it is only very recently that the resulting X-ray emission from highly charged ions in the wind has been considered. The basic process in CX is the radiationless collisional transfer of one or sometimes multiple electrons from a neutral atom or molecule to an ion. Electron transfer can also occur between two ions, but Coulombic repulsion greatly reduces the interaction cross section. The recipient ion is, for X-ray–emitting highly charged ions, left in a high-n excited state, which then decays via single or sequential radiative transitions.

The first astrophysical observation of such X-ray emission was from comets (Lisse et al. 1996; Dennerl, Englhauser, & Trümper 1997). As first proposed by Cravens (1997), these X-rays are produced via the charge exchange of highly charged solar wind ions with neutral atoms and molecules in the comet's atmosphere. Subsequent papers (Häberli et al. 1997; Krasnopolsky 1997; Wegmann et al. 1998; Lisse et al. 1999; Neugebauer et al. 2000; Schwadron & Cravens 2000; Kharchenko

& Dalgarno 2000) have supported and expanded that idea and have included detailed models of the expected X-ray spectrum (Kharchenko & Dalgarno 2000), which is dominated from 200 to 1000 eV by K shell emission from H-like and He-like ions of C, O, N, and Ne. Recent *Chandra* observations of comet C/1999 S4 (LINEAR) by Lisse et al. (2000) detected prominent O VII emission at 570 eV along with several other weaker lines, providing strong evidence that CX is indeed the dominant X-ray emission mechanism.

Following the observation of cometary X-rays, Cox (1998) suggested that X-rays should also be produced from CX of the solar wind with neutral gas streaming into the heliosphere from the ISM. Using a fairly conservative model, Cravens (2000) estimated that this mechanism accounts for about 25%–50% of the observed soft X-ray background below roughly 0.5 keV. This is consistent with data from the Wisconsin soft X-ray background sky survey (McCammon & Sanders 1990) and *ROSAT* observations (Snowden et al. 1994, 1995, 1998), which suggest that roughly half of the $\frac{1}{4}$ keV background emission comes from a "local hot plasma." Cravens also pointed out that temporal variations seen in the *ROSAT* data are similar to what would be expected from CX X-ray emission caused by variations in the solar wind, further strengthening a heliospheric interpretation.

This same process must occur for all stars with highly charged winds, and we show that large-area high-resolution observatories such as *Chandra* should be capable of detecting winds that are only moderately stronger than the Sun's, corresponding to mass-loss rates orders of magnitude smaller than have been previously measurable.

3. EMISSION FROM STELLAR WINDS

As most recently noted by Kharchenko & Dalgarno (2000), the rate of CX emission is higher at energies below 200 eV than above 300 eV because only the most highly charged ions emit photons at X-ray energies, while virtually all metal ions in the solar wind emit at extreme ultraviolet energies and below. From the viewpoint of detecting CX/wind emission, however, the higher energy photons are easier to see because of their higher contrast with emission from the central star.

In addition, useful spectral information can be obtained at X-ray energies with nondispersive detectors, unlike at lower energies. Nevertheless, extreme UV observations might be very revealing, but no EUV missions to date have had the requisite combination of large collecting area, high spatial resolution, and low detector background.

The following discussion focuses on CX emission from He-like O VII, which is the brightest component of solar-cometary X-ray spectra and likely to be so in other stellar systems. The population of bare and H-like C ions in the solar wind is actually larger than for O (von Steiger et al. 1992), but X-ray emission from C lies between about 300 and 400 eV, in an energy range where detection efficiency is very poor because of the nearly inescapable use of thin plastic windows and filters in X-ray detectors. The carbon in these filters is strongly absorbing at energies just above 284 eV, with the result that detected O emission is much stronger than that from C.

Another reason to focus on O VII CX emission is that it is dominated by Kα photons, allowing a tight energy-filtering range to be applied to observational data and significantly reducing the effective detector background in what will generally be photon-starved observations. As explained by Beiersdorfer et al. (2000), CX populates high-n levels in He-like ions such as O VII, but the coupling of the two electrons' spins means that an $S = 1$ (triplet) state occurs about 3 times as often as an $S = 0$ (singlet) state. The $\Delta S = 0$ selection rule prohibits dipole decay of the $1snl$ triplet states to the singlet $1s^2\,{}^1S_0$ ground, resulting in radiative cascades to $1s2l$ triplet levels, which then decay via higher multipole radiation to ground and emit Kα emission. Likewise, a significant fraction of the original singlet states cannot decay directly to ground because of other selection rules (such as $\Delta l = \pm 1$), so that nearly all the He-like X-ray emission is from $n = 2 \rightarrow 1$ transitions. CX emission from H-like ions, in contrast, has a much higher fraction of decays from high-n levels directly to ground because there are no spin-change radiative constraints, thus spreading the emission over a broader energy range.

3.1. *Modeling the CX Emission Distribution*

The CX emissivity (in units of photons s^{-1} cm^{-3}) of any ion is given by

$$\epsilon = n_{\rm H} n_{\rm ion} v_{\rm ion} \sigma_{\rm CX}, \tag{1}$$

where $n_{\rm H}$ is the neutral gas density, $n_{\rm ion}$ is the density of the "parent" ion, $v_{\rm ion}$ is the collision velocity, and $\sigma_{\rm CX}$ is the CX cross section. We have set the center-of-mass collision velocity equal to the velocity of the ion since the neutral gas atoms are less massive and generally much slower. Note that *every* CX collision with a highly charged ion produces an X-ray and lowers the ion charge.

We begin a quantitative assessment of stellar wind/CX emission by considering the solar wind, approximating it as being spherically symmetric and purely radial, with no attempt to include the effects of shocks and asymmetries within and beyond the heliosphere. Since, as will be shown, the bulk of the CX emission occurs within the roughly 100 AU radius heliosphere and is concentrated toward the center, this simplification has no significant impact on our main conclusions.

We model the density of neutral gas as $n_{\rm H} = n_{\rm H_0} \times \exp(-\lambda_{\rm H}/r)$, where r is the distance from the Sun, $n_{\rm H_0}$ is the neutral gas density at large values of r (0.15 cm^{-3}), and $\lambda_{\rm H}$ is the scale length for depletion of neutral H near the Sun, primarily by CX with solar wind protons but also by photoionization, etc. In that simple model used by Cravens (2000), $\lambda_{\rm H}$ is roughly 20 AU on the "downstream" side of the Sun's motion through the ISM, but we use the upstream value of 5 AU here. The significance of $\lambda_{\rm H}$ will be discussed later, but its exact value is of minor importance in our calculations for the Sun.

The product of $n_{\rm ion}(r)$ and $v_{\rm ion}(r)$ is equal to the particle flux (particles per second) divided by $4\pi r^2$. At 1 AU the wind density is approximately 7 cm^{-3} with an average velocity of 400 km s^{-1}. The flux of solar wind O ions is equal to the solar mass-loss rate, roughly $2 \times 10^{-14}\,M_\odot$ yr^{-1}, times the fractional abundance of the ion. For O ion abundances we use the values recommended by Kharchenko & Dalgarno (2000) after their search of the literature: 5.3×10^{-4} for oxygen abundance relative to hydrogen, with 0.09 and 0.24 for the fractions of bare and H-like oxygen ions, respectively. This yields a rate of 3.6×10^{31} O IX ions and 9.6×10^{31} O VIII ions per second injected into the solar wind.

No measurements of cross sections for CX between highly charged O ions and H, He, or H_2 are available, but Greenwood et al. (2000) have recently measured cross sections for CX with H_2O and CO_2 at energies somewhat higher than those found in the solar wind and obtained typical values of 6×10^{-15} cm^2 for single-electron transfer. Phaneuf et al. (1982) measured

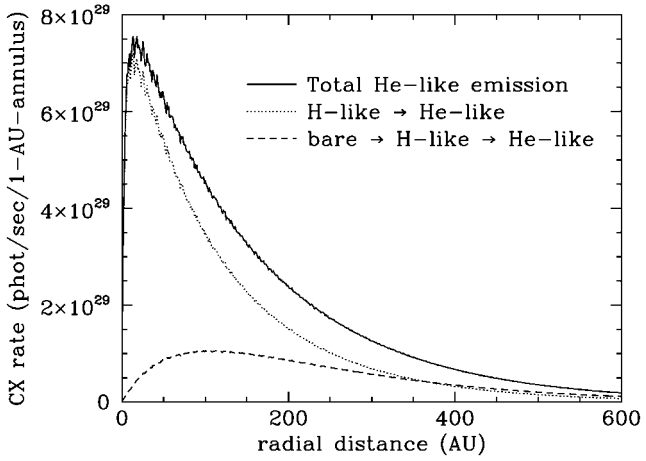

FIG. 1.—Model solar wind CX emission from He-like O VII, as would be observed from afar, in 1 AU annular bins. Choppiness in the curves is an artifact of the grid used in the simulation. [*See the electronic edition of the Journal for a color version of this figure.*]

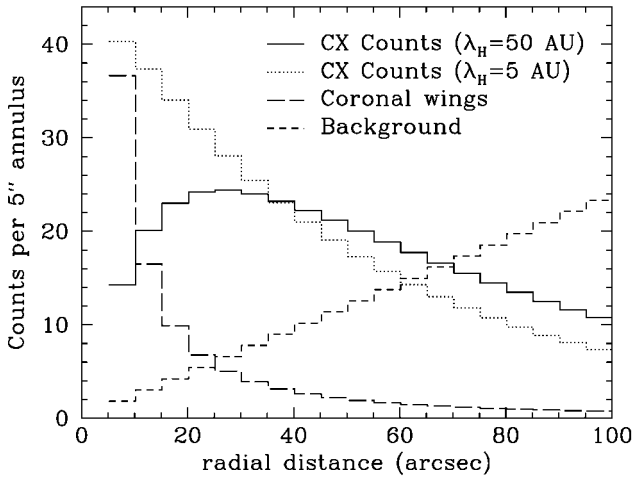

FIG. 2.—Simulation of O VII CX emission from 100 times solar stellar wind at a distance of 3 pc, observed with *Chandra* ACIS-S detector for 100 ks, with 5″ annular binning (corresponding to 15 AU). Results are shown for two different values of λ_H, the length scale for neutral H depletion near the star. Wings from the central coronal emission are shown assuming a detected rate of 0.1 counts s^{-1} in the O Kα energy band.[*See the electronic edition of the Journal for a color version of this figure.*]

cross sections for CX of various O (and C) ions with H and H_2, but only up to Li-like O VI. We adopt the estimated value of $\sim 3 \times 10^{-15}$ cm^2 used by Cravens (2000) and others for CX of O VII and O VIII with neutral H atoms. With a neutral H density of 0.15 cm^{-3} for the local ISM, the path length for CX collisions, $\lambda_{CX} = 1/(n_H \sigma_{CX})$, is therefore roughly 150 AU. Radiative recombination is of negligible importance because of its much smaller cross section and the low electron density.

Emissivity is computed numerically using equation (1) as a function of radial distance from the Sun, starting at 1 AU and extending out to 1000 AU in 1 AU steps. Note that because fully ionized O IX ions contribute to He-like X-ray emission via sequential CX to H-like O VIII and then He-like O VII, the densities of both O IX and O VIII ions must be computed. The relevant equations are

$$\frac{dn_{\rm IX}(r)}{dr} = \left[-\frac{2}{r} - \frac{1}{\lambda_{\rm CX}(r)}\right] n_{\rm IX}(r), \tag{2}$$

$$\frac{dn_{\rm VIII}(r)}{dr} = \left[-\frac{2}{r} - \frac{1}{\lambda_{\rm CX}(r)}\right] n_{\rm VIII}(r) + \frac{1}{\lambda_{\rm CX}(r)} n_{\rm IX}(r). \tag{3}$$

The $-2/r$ terms reflect the $1/r^2$ dependence of the wind density, while the $1/\lambda_{CX}$ terms represent the depletion or addition of specific ions via CX collisions. Note that λ_{CX} is a function of r because of its dependence on n_H, which is depleted near the Sun.

The results computed above are interpolated to determine the emissivity at every point in a 1000 AU radius octant of three-dimensional space with 1 AU grid spacing. The emission is then collapsed into two dimensions, as it would appear on the sky when observed far from the Sun, and finally divided into radial (annular) bins. Figure 1 shows the resulting distribution of X-ray emission from He-like O VII and the individual contributions from the parent O IX and O VIII ions.

3.2. *Detectability of Nearby Stellar Winds*

Now consider a star with a wind 100 times stronger than the Sun at a distance d of 3 pc observed with the Advanced CCD Imaging Spectrometer-S (ACIS-S) detector on the *Chandra X-Ray Observatory* for $t = 100$ ks. Since essentially every bare and H-like O ion will eventually emit a He-like X-ray, the O VII emission rate $R_{\rm phot}$ will be $100 \times (3.6 \times 10^{31} + 9.6 \times 10^{31}) = 1.32 \times 10^{34}$ photons s^{-1}. With an effective area A of roughly 400 cm^2 at 570 eV (*Chandra* Proposers' Observatory Guide [POG]), the number of detected Kα counts, given by

$$N_{\rm det} = \frac{R_{\rm phot} A t}{4\pi d^2}, \tag{4}$$

will be close to 500, nearly all of which will be detected at radii greater than 5″ from the star. At smaller radii, coronal emission from the star would likely swamp the CX signal.

Figure 2 shows the distribution of Kα counts with 5″ radial binning, using two values of λ_H (5 and 50 AU). The larger value is roughly appropriate for our example 100 times solar wind; proton-hydrogen CX will tend to sweep out a larger volume of neutral gas, with λ_H scaling as roughly $\dot{M}^{1/2}$. Higher fluxes of ionizing radiation will also increase the extent of neutral gas depletion. The histogram using the smaller value of 5 AU is shown to illustrate the effect of different values of λ_H.

The background signal is based on a rate of 1.5×10^{-7} counts s^{-1} arcsec^{-2} within a 200 eV–wide energy band centered on 570 eV (*Chandra* POG; M. Markevitch 2000, private communication). Coronal emission from the central star is shown assuming a pessimistically high rate of 0.1 counts s^{-1} within the same energy band. *Chandra*'s spatial resolution is extremely high (FWHM $\leq$ 0.″5), with a surface brightness distribution that falls off as $r^{-2.5}$ (*Chandra* POG), so that only about 130 of the 10,000 coronal counts fall more than 5″ from the center. The net signal-to-noise ratio (S/N), $N_{\rm CX}/(N_{\rm CX} + N_{\rm BG} + N_{\rm wings})^{1/2}$, is larger than 3 out to radii of more than 50″.

Coarser radial binning will increase the S/N somewhat. All other things being equal, the number of detected CX counts goes as the inverse square of the distance to a star, but the angular size of the emission region scales as $1/d$ so that the number of detected photons per radial bin (counts per arcsecond) is roughly proportional to $1/d$. For our example of a 100

times solar wind at 3 pc, the S/N is mostly determined by the number of CX counts out to several tens of arcseconds and therefore scales as roughly $(N_{CX})^{1/2}$, so that the S/N is greater than 2 even for CX emission that is several times weaker. Likewise, the example wind can be seen at distances well beyond 10 pc.

So far we have considered only He-like O VII emission. Given a typical detector CCD energy resolution of roughly 150 eV (FWHM), much of the signal from H-like O VIII (at $E \geq 654$ eV) and N VII (at $E \geq 500$ eV) will be detected within our example 470–670 eV energy band. In more highly ionized winds there will be a higher fraction of these X-ray–emitting ions, and L shell emission from intermediate-charge Fe ions will also contribute. In most cases the S/N will be further improved by using a wider energy band to include emission from more ions. As Cravens (2000) suggests (for the solar case), there may also be enhanced emission at large radii because of the higher neutral gas density near the astropause and the higher wind density in the shocked flow.

4. APPLICATIONS

There are many candidates for stellar wind/CX observations with *Chandra* or future large-area high-resolution X-ray missions. The dMe stars are of particular interest because of their ubiquity and because one might expect flaring M stars to have stronger winds than their nonactive counterparts. Their winds are also likely to be more highly ionized than the Sun's because of higher coronal temperatures, which are up to an order of magnitude higher than the solar value of $T \sim 2 \times 10^6$ K (Schmitt et al. 1990). Within 5 pc there are 19 X-ray–detected dMe stars, out of 42 M stars in the *ROSAT* survey (Wood et al. 1994), plus over a dozen A, F, G, and K stars, of which most are K type. Within 3 pc, six of the seven M stars are classified as flaring.

Detection of such stars' wind-driven CX X-ray emission would provide sorely needed insight into dwarf star winds and their interaction with the ISM. In addition to basic information on mass-loss rates, other things that could be studied are stellar wind geometry, providing information on polar versus equatorial flows, coronal mass ejections, and other spatial and temporal variability; astrosphere geometry, from observations of emission on the leading and trailing edges of stellar motion through the ISM (Wood & Linsky 1998); and correlations between wind characteristics and metallicity, coronal emission, flaring activity, and stellar type.

The distribution of neutral gas in the local ISM could also be investigated. The Sun is believed to lie within and near the boundary of a high-density local interstellar cloud (LIC; Holzer 1989); for stars lying in low-density regions of the ISM, the path length for CX would be at least several hundred parsecs, and so their CX/wind emission would be spread out over a much larger volume, rendering it undetectable. Likewise, the detection of a stellar wind would almost certainly imply that the star lies within the LIC or other region of enhanced density.

The heavy-ion composition of stellar winds could also be inferred from spectra, particularly on future missions employing microcalorimeter technology. Detectors such as the X-Ray Spectrometer (Kelley et al. 1999) built for the *Astro-E* mission have energy resolution of better than 10 eV FWHM at soft X-ray energies, which is more than adequate to distinguish between the emission from different ions.

One could also determine wind velocities by measuring hardness ratios in H-like spectra (high-n transitions vs. $n = 2 \rightarrow 1$ lines). As explained by Beiersdorfer et al. (2000) and experimentally demonstrated for elements including Ar and Xe, the absence of spin-coupling effects in H-like ions means that electrons captured into high-n states with $l = 1$ can decay directly to the $l = 0$ ground state. The hardness ratio therefore depends on the angular momentum of the electron captured by CX, which has a probability distribution that is a function of collision velocity at energies similar to those in the solar wind.

Even if wind/CX emission is not detected, much firmer limits can be placed on stellar wind properties than has been possible up to now. As noted earlier, a mass-loss rate of several times $10^{-13}\ M_\odot\ \mathrm{yr}^{-1}$, which is roughly 1000 times lower than has been previously detected, should be observable out to several parsecs for stellar winds having solar-type wind composition, and more highly ionized winds will be even brighter.

The authors were supported by NASA contract NAS8-39073 to the *Chandra* X-Ray Center during the course of this research.

REFERENCES

Badalyan, O. G., & Livshits, M. A. 1992, Soviet Astron., 36, 70
Beiersdorfer, P., et al. 2000, Phys. Rev. Lett., 85, 5090
Brown, A., Vealé, A., Judge, P., Bookbinder, J. A., & Hubeny, I. 1990, ApJ, 361, 220
Coleman, G. D., & Worden, S. P. 1977, ApJ, 218, 792
Cox, D. P. 1998, in The Local Bubble and Beyond, ed. D. Breitschwerdt, M. J. Freyberg, & J. Trümper (Berlin: Springer), 121
Cravens, T. E. 1997, Geophys. Res. Lett., 24, 105
———. 2000, ApJ, 532, L153
Dennerl, K., Englhauser, J., & Trümper, J. 1997, Science, 277, 1625
Greenwood, J. B., Williams, I. D., Smith, S. J., & Chutjian, A. 2000, ApJ, 533, L175
Häberli, R. M., Gombosi, T. I., de Zeeuw, D. L., Combi, M. R., & Powell, K. G. 1997, Science, 276, 939
Holzer, T. E. 1989, ARA&A, 27, 199
Kelley, R., et al. 1999, Proc. SPIE, 3765, 114
Kharchenko, V., & Dalgarno, A. 2000, J. Geophys. Res., 105, 18,351
Krasnopolsky, V. 1997, Icarus, 128, 368
Krishnamurthi, A., Pinsonneault, M. H., Barnes, S., & Sofia, S. 1997, ApJ, 480, 303
Lamers, H. J. G. L. M., & Cassinelli, J. P. 1999, Introduction to Stellar Winds (Cambridge: Cambridge Univ. Press)
Lim, J., & White, S. M. 1996, ApJ, 462, L91
Lisse, C. M., et al. 1996, Science, 274, 205
———. 1999, Icarus, 141, 316
Lisse, C. M., et al. 2000, IAU Circ. 7464
McCammon, D., & Sanders, W. T. 1990, ARA&A, 28, 657
Mullan, D. J., Doyle, J. G., Redman, R. O., & Mathioudakis, M. 1992, ApJ, 397, 225
Neugebauer, N., Cravens, T. E., Lisse, C. M., Ipavich, F. M., von Steiger, R., Shah, P. D., & Armstrong, T. P. 2000, J. Geophys. Res., 105, 2315
Phaneuf, R. A., Alvarez, I., Meyer, F. W., & Crandall, D. H. 1982, Phys. Rev. A, 26, 1892
Schmitt, J. H. M. M., Collura, A., Sciortino, S., Vaiana, G. S., Harnden, F. R., Jr., & Rosner, R. 1990, ApJ, 365, 704
Schwadron, N., & Cravens, T. E. 2000, ApJ, 544, 558
Smith, G. H. 1999, PASP, 111, 980
Snowden, S. L., et al. 1994, ApJ, 424, 714
———. 1995, ApJ, 454, 643
———. 1998, ApJ, 493, 715
van den Oord, G. H. J., & Doyle, J. G. 1997, A&A, 319, 578
von Steiger, R., Christon, S., Gloeckler, G., & Ipavich, F. M. 1992, ApJ, 389, 791
Wegmann, R., Schmidt, H. U., Lisse, C. M., Dennerl, K., & Englhauser, J. 1998, Planet. Space Sci., 46, 603
Willson, L. A., Bowen, G. H., & Struck-Marcell, C. 1987, Comments Astrophys., 12, 17
Wood, B. E., Brown, A., Linsky, J. L., Kellet, B. J., Bromage, G. E., Hodgkin, S. T., & Pye, J. P. 1994, ApJS, 93, 287
Wood, B. E., & Linsky, J. L. 1998, ApJ, 492, 788